Yield strength enhancement of MgO by nanocrystals

JEDDY CHEN[†], NATHAN SCHMIDT[‡], JIUHUA CHEN, LIPING WANG, DONALD J. WEIDNER[*]
Mineral Physics Institute, State University of New York at Stony Brook, Stony Brook, NY 11794-2100, USA
E-mail: dweidner@notes.cc.sunysb.edu

JIANZHONG ZHANG
Los Alamos National Laboratory, Los Alamos, New Mexico, USA

YANBIN WANG
The Consortium for Advanced Radiation Sources, University of Chicago, Chicago, Illinois, USA

Published online: 20 September 2005

Behaviors of nanomaterials have been increasingly attracting the interests of scientific and industrial researchers in the past decade because many of their properties—such as magnetism, catalysis, and optics—are very distinct from predictions based on the behavior of coarse materials [1–8]. The study of nanomaterials' properties therefore holds the promise of revolutionizing traditional materials' design in many applications. On the other hand, the predicted behaviors of materials at the nanometer-scale based on the properties of coarse materials are sometimes more desirable; which includes changes in the mechanical properties at the nanometer scale. Here we report an experimental result on comparative studies of yield strengths of nano-size and micron-size MgO crystals by using energy dispersive powder X-ray diffraction. Our study indicates a significant enhancement of yield strength in nanocrystal MgO: yield strength of MgO with 10 nm average crystal size is about 35% higher than that with 1 mm average grain size.

Traditionally for most metals, the mechanical strength σ is believed to be largely controlled by the grain size P, following the Hall-Petch relation [9, 10]

$$\sigma = kP^{-1/2} + \sigma_0$$

where k and σ_0 are experimentally determined constants, due to the grain boundary enhanced obstacles on the generation and/or motion of dislocation. This relation predicts great increases in strength as grain size decreases to the nanometer scale. However, theoretical studies indicate that the high volume fraction of interfacial regions results in significant deformation by grain boundary sliding in metals at very small grain sizes, only tens of nanometers [11]. Furthermore, a computer simulation of the deformation of nanocrystalline copper actually shows a reverse Hall-Petch effect (softening with decreasing grain size) [12]. Experimentally, both normal and reverse Hall-Petch effects have been observed in some metals and alloys [13–19]. As the strength measurements were carried out on bulk sample made of nanosize grains, the reverse Hall-Petch effect was attributed to increased porosity at small grain sizes from experimental point of view [13, 19]. However, some measurements with improved dense-specimen still show a tendency of softening at very small grain sizes [13, 20–22]. The study of the mechanical property of nanocrystalline oxides is much less extensive than that of metals and alloys. A significant inconsistency to the normal Hall-Petch effect has been observed in sintered bulk specimens of TiO_2 [23–25] as the grain size decreased from coarse grain to the nanometer size. Here we report an application of energy dispersive X-ray diffraction to measure both the average differential stress and the grain size of powdered MgO, and the result indicates a significant increase in MgO yield strength as its grain (crystal) size decreases from micrometers to nanometers.

The experiments were conducted using the synchrotron X-ray beamline X17B [26] at the National Synchrotron Light Source and the GSECARS [27] at the Advanced Photon Source. High purity (99.99%) powdered MgO sample was packed (1 mm in diameter and 0.5–1.0 mm in length) into a pressure cell and was subjected to loading in a multi-anvil press [26]. Upon loading, grain-to-grain contacts generated elastic differential strain (grain distortion) amongst themselves, in addition to the hydrostatic compression [28]. This elastic strain increases linearly with load until the stress for generating such strain reaches the yield strength of the grains. As the load was increased stepwise, in-situ X-ray diffraction patterns were taken using a white X-ray beam with an energy range of 20–120 keV and a size of 100 μm × 100 μm to monitor the elastic strain and grain size. The differential stain and the small crystal size are the two major causes of line broadening

[*]Author to whom all correspondence should be addressed.
[†]Research Intern from Ward Melville High School, Setauket, New York, USA.
[‡]Summer Research Scholar from Macalester College, St Paul, Minnesota, USA.

0022-2461
DOI: 10.1007/s10853-005-2476-8

in X-ray diffraction pattern of powder samples [29]. The diffraction peak width (B: FWHM—full width at half maximum) is described as [30, 31] $B^2 - B_i^2 = B_d^2 + B_s^2$ where B_i is the instrumental broadening, B_d is the differential strain broadening, and B_s is the grain size broadening. In the case of energy dispersive diffraction [32] $B_d = 2eE$ and $B_s = K(\frac{1}{2}hc)/(P \sin\theta_0)$ (K: Scherrer constant, h: Planck's constant, c: the velocity of light, P: the average grain size, $2\theta_0$: the fixed scattering angle, e: the average elastic differential strain, E: the X-ray photon energy). As the instrumental broadening can be measured using a strain-free sample with a nearly ideal grain size ($\sim$1 μm), the differential strain and grain size are derived by fitting the peak broadening (B^2–B_i^2) of all observed peaks in a diffraction pattern to a linear equation as a function of the photon energy (E^2) of each peak. For a conventional energy dispersive diffraction setup ($2\theta_0 \sim 7^\circ$), $K(^1/_2)hc/\sin\theta_0 =$ 91.5 keV nm. The high energy resolution ($R = 200$ eV) of the Ge solid state detector used in this study sets an upper limit of $\sim$500 nm for accurate grain size measurements.

The measurements were conducted on two samples with average grain size of 30 nm (from Nanopowder Enterprises Inc.) and 1 μm (from Alfa Aesar) respectively. Fig. 1a illustrates the broadening of diffraction peaks in the diffraction patterns of the nano-grain-size sample as it is compressed. Three diffraction peaks (111), (200) and (220) are used in deriving average grain size and stress for the nano-grain-size sample, whereas two additional peaks (311) and (222) are also used for the micro-grain-size sample because the diffraction patterns were of a higher quality. Fig. 1b shows the peak broadening (B^2–B_i^2) of (111), (200) and (220) as a function of photon energy (E^2) in the diffraction patterns of the nano-grain-size sample at ambient condition, load = 2.3×10^5 N and load = 8.2×10^5 N respectively. Each set of data can be fit into a linear function, and differences in the slope and y-intercept of the linear function at different conditions are caused by the change of grain size and differential stress of the sample, respectively. Upon loading, the samples experienced a slight grain size reduction (Fig. 2). The average grain size of nano-sample reached $\sim$10 nm. The grain size variation in micron-sample could not be accurately measured due to the limitation of detector resolution, but measurements indicate that the gain size was greater than 500 nm throughout the experiment. Fig. 3 shows the derived differential stresses (product of differential strain and Young's modulus) in the two samples as a function of load. Stresses in both

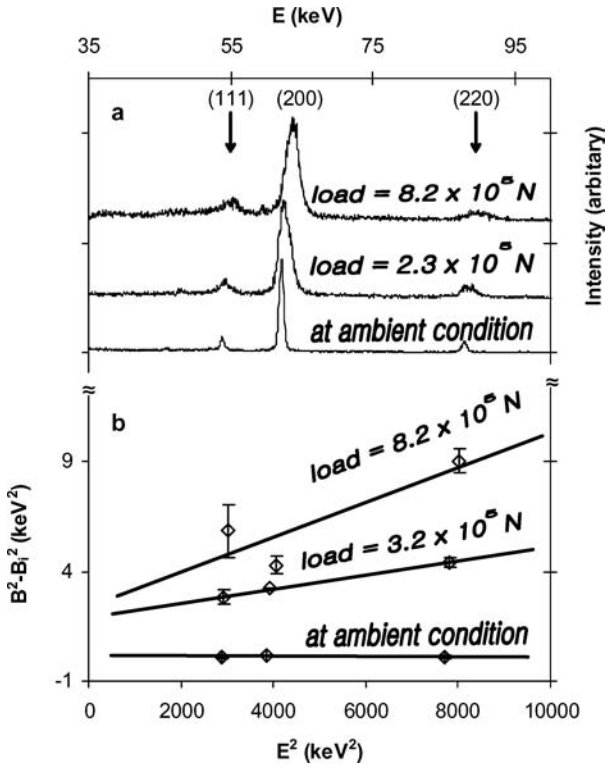

Figure 1 (**a**) Powder X-ray diffraction patterns (Intensity—left axis *vs.* Energy—top axis) of nano-grain-size MgO before and during loading. Significant peak broadening is observed once the sample is under loading. (b) Diffraction peak broadening (B^2-B_i^2—right axis) as a function of energy (E^2—bottom axis). Solid lines represent a linear fit to each data set. Increase in the slope of the linear function upon loading is caused by internal stress. Bars attached to the symbols represent experimental uncertainties.

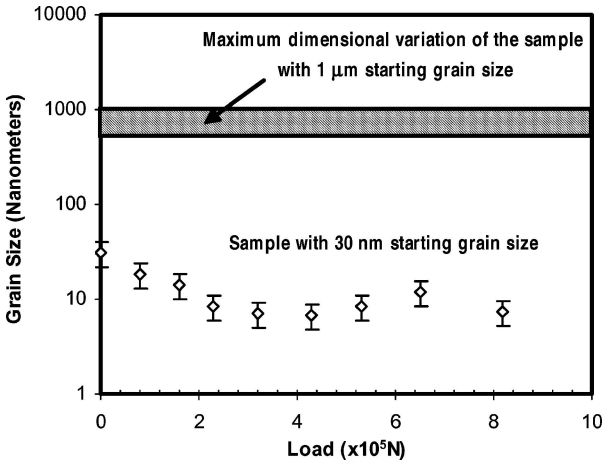

Figure 2 Variation of grain sizes during loading. Diamond symbols represent the average grain sizes of the nano-sample derived from X-ray diffraction using Warren-Averbach method. The shaded area indicates the maximum variation in grain size of the micron-sample, due to limited resolution of Warren-Averbach method for large grain size. Bars attached to the symbols represent experimental uncertainties.

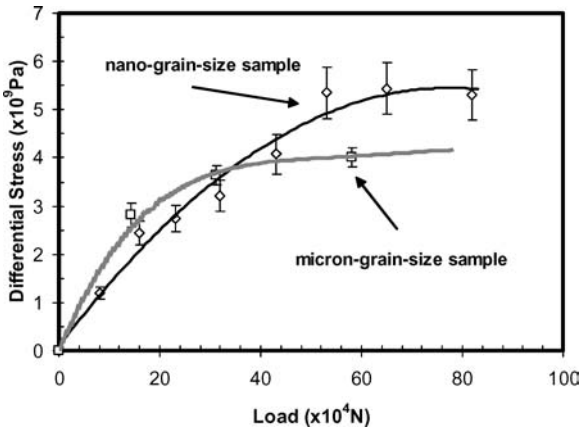

Figure 3 Differential stress in micron-grain-size sample (open squares) and nano-grain-size sample (open diamonds) as a function of load. Bars attached to the symbols represent experimental uncertainties. Lines are drawn just for easy recognition of yielding.

samples increased rapidly as the load increased before the stress reached the yield strength of each sample. Once the sample began to yield (the stress reached the strength of the sample), stress in the sample did not increase even with further increases of load. The micron-grain-size sample yielded when the differential stress reached 4 ± 0.3 GPa, whereas the nano-grain-size sample did not yield until the differential stress reached 5.4 ± 0.3 GPa. Beyond this yield point, the stress vs. load curve of each sample approached a plateau. This result demonstrates a significant increase (35%) in the yield strength in MgO as the grain size was decreased from about 1 μm to 10 nm.

In these experiments, the two samples had very distinct grain sizes (1 μm vs. 10 nm). While observations from the two samples clearly demonstrate an enhancement of yield strength by reduction of grain size, further systematic measurements of yield strength as a function of grain size are essential to reveal grain-size dependence of yield strength of MgO at a finer scale. If we fitted the Hall-Petch relation $\sigma = kP^{-1/2} + \sigma_0$ to the current two data points, the constants k and σ_0 were estimated to be $k = 4.9$ GPa·nm$^{1/2}$ and $\sigma_0 = 3.8$ GPa. Hulse *et al.* [33]. studied the plastic deformation of single crystal MgO and their results indicates that the single crystal MgO with the (111) loading axis is much stronger than those with other orientations, with a yield strength greater than 3.6 GPa. In Hall-Patch relation, σ_0 can be considered as the strength when the grain size approaches infinity. The derived value of σ_0 from our experiment is consistent with the single crystal data along the strong orientation of MgO.

The study reported here is a direct measurement of the average yield strength for individual grains using X-ray diffraction, which avoids the influence of a bulk sample quality (porosity) on indentation or deformation experiments. This method has been widely used in measuring residual stresses in materials [34]. The technique was extended here to measure the stress in a powder sample during loading. Since stresses are generated by grain-to-grain contact (self-indentation), the method has been applied to measure the strength of superhard materials, such as diamond [35] and moissanite [36], as well as materials that are stable only at high pressures [37]. Measurement of grain sizes using X-ray diffraction is also a classic technique in material studies. This technique is often referred as Warren-Averbach method [31, 38], and used to measure the average grain size of nanocrystalline metal samples [21]. For the first time, we simultaneously measured the stress and grain size during loading on the sample to study the grain-size dependence of the yield strength using X-ray diffraction.

Acknowledgements

This work was supported by research and education grants of the National Science Foundation and the U.S. Department of Energy. The National Synchrotron Light Source and Advanced photon source are supported by Department of Energy. The high pressure beamline X17B at NSLS is supported by COMPRES and SUNY at Stony Brook. GSECARS at APS is supported by the National Science Foundation, Department of Energy, W. M. Keck Foundation, and the U.S. Department of Agriculture. We thank Drs. M. T. Vaughan, Z. Zhong and T. Uchida for their help in the data collection at NSLS and APS. MPI pub number 357.

References

1. J. KUMA, N. KITAJIMA, Y. KANAI and H. FUKUNAGA, *J. Appl. Phys.* **83** (1998) 6623.
2. G. A. PRINZ, *Science* **282** (1998) 1660.
3. R. NOTZEL, *Microelectr. J.* **28** (1997) 875.
4. J. LI, A. MIRABEDINI, L. J. MAWST, D. E. SAVAGE, R. J. MATYI and T. F. KUECH, *J. Cryst. Growth* **195** (1998) 617.
5. A. HEMMERICH and T. W. HANSCH, *Phys. Rev. Lett.* **70** (1993) 410.
6. M. M. BURNS, J.-M. FOURNIER and J. A. GOLOVCHENKO, *Science* **249** (1990) 749.
7. M. SASAKI, M. OSADA, N. SUGIMOTO, S. INAGAKI, Y. FUKUSHIMA, A. FUKUOKA and M. ICHIKAWA, *Microporous. and Mesoporous. Mater.* **21** (1998) 597.
8. S. C. SHEN, K. HIDAJAT, L. E. YU and S. KAWI, *Catal. Today* **98** (2004) 387.
9. E. O. HALL, *Proc. Phys. Soc. Lond. B* **64** (1951) 747.
10. N. J. PETCH, *J. Iron Steel Inst.* **174** (1953) 25.
11. R. L. COBLE, *J. Appl. Phys.* **34** (1963) 1679.
12. J. SCHIØTZ, F. D. D. TOLLA and K. JACOBSEN, *Nature* **391** (1998) 561.
13. R. W. SIEGEL and G. E. FOUGERE, in "Nanophase Materials: Synthesis-Properties-Applications," edited by G. C. Hadjipanayis and R. W. Siegel (Kluwer: Dordrecht, 1994) p. 233.
14. G. W. NIEMAN, J. R. WEERTMAN and R. W. SIEGEL, *J. Mater. Res.* **6** (1991) 1012.
15. G. E. FOUGERE, J. R. WEERTMAN, R. W. SIEGEL and S. KIM, *Scripta Metall. Mater.* **26** (1992) 1879.
16. K. LU, W. D. WEI and J. T. WANG, *ibid.* **24** (1990) 2319.
17. A. H. CHOKSHI, A. ROSEN, J. KARCH and H. GLEITER, *Scripta Metall.* **23** (1989) 1679.
18. G. W. NIEMAN, J. R. WEERTMAN and R. W. SIEGEL, *ibid.* **23** (1989) 2013.
19. P. G. SANDERS, C. J. YOUNGDAHL and J. R. WEERTMAN, *Mater. Sci. Enging.* **A234** (1997) 77.
20. P. G. SANDERS, J. A. EASTMAN and J. R. WEERTMAN, *Acta Mater.* **45** (1997) 4019.
21. J. R. WEERTMAN, D. FARKAS, K. HEMKER, H. KUNG, M. MAYO, R. MITRA and H. V. SWYGENHOVEN, *MRS Bulletin* **24** (1999) 44.
22. R. W. SIEGEL, *J. Phys. Chem. Solids* **55** (1994) 1097.
23. R. S. AVERBACK, H. J. HÖFLER, H. HAHN and J. C. LOGAS, *Nanostruct. Mater.* **1** (1992) 173.
24. M. GUERMAZI, H. J. HÖFLER, H. HAHN and R. S. AVERBACK, *J. Am. Ceram. Soc.* **74** (1991) 2672.
25. H. J. HÖFLER and R. S. AVERBACK, *Script Metall. Mater.* **24** (1990) 2401.
26. D. J. WEIDNER, M. T. VAUGHAN, J. KO, Y. WANG, X. LIU, A. YEGANEH-HAERI, R. E. PACALO and Y. ZHAO, "High-pressure research: Application to Earth and planetary sciences," edited by Y. Synono and M. H. Manghnani (Terra Scientific Publishing Company, AGU: Tokyo, Washington, D.C., 1992) p. 13.
27. Y. WANG, M. L. RIVERS, T. UCHIDA, P. MURRAY, G. SHEN, S. SUTTON, J. CHEN, Y. XU and D. WEIDNER, "Science and Technology of High Pressure," edited by W. J. N. M. H. Manghnani and M. F. Nicol (Universities Press Ltd.: Hyderabad, 2000) p. 1047.
28. D. J. WEIDNER, Y. WANG, G. CHEN, J. ANDO and M. T. VAUGHAN, *Prop. Earth Planet. Mater. High Press. Temper.* (1998) p. 473.
29. F. W. WILLETS, *Brit. J. Appl. Phys.* **16** (1965) 323.
30. H. P. KLUG and L. E. ALEXANDER, in "Series X-ray Diffraction Procedures" (Wiley: New York, 1974).

31. B. WARREN, in "Series X-ray Diffraction," (Addison-Wesley: London, 1989).
32. L. GERWARD, S. MORUP and H. TOPSOE, *J. Appl. Phys.* **47** (1976) 822.
33. C. O. HULSE, S. M. COPLEY and J. A. PASK, *J. Am. Ceram. Soc.* **46** (1963) 317.
34. A. D. WESTWOOD, C. E. MURRAY and I. C. NOYAN, "Advances in X-ray Analysis" **38** (1995) 243.
35. D. J. WEIDNER, Y. WANG and M. T. VAUGHAN, *Science* **266** (1994) 419.
36. J. ZHANG, L. WANG, D. J. WEIDNER, T. UCHIDA and J.-A. XU, *Amer. Mineral.* **87** (2002) 1005.
37. J. H. CHEN, D. J. WEIDNER and M. T. VAUGHAN, *Nature* **419** (2002) 824.
38. B. E. WARREN and B. L. AVERBACH, *J. Appl. Phys.* **23** (1952) 497.

Received 8 April
and accepted 24 May 2005